

A GaN-Based Lamb-Wave Oscillator on Silicon for High-Temperature Integrated Sensors

Xing Lu, Jun Ma, C. Patrick Yue, *Senior Member, IEEE*, and Kei May Lau, *Fellow, IEEE*

Abstract—This letter presents the first fully integrated GaN-based Lamb-wave oscillator on Si substrate for high temperature operation. The 58 MHz oscillator prototype was implemented by monolithically integrating a two-port Lamb-wave delay line with electronics using AlGaIn/GaN high electron mobility transistors (HEMTs). Electrical characterization from room temperature (RT) up to 250°C was performed on the open-loop Lamb-wave delay line device and the integrated oscillator. It is shown that this oscillator is able to deliver high output power (>11 dBm) up to 250°C. Over the temperature range from RT to 230°C, the oscillation frequency exhibits a linear dependence on temperature with a small temperature coefficient of frequency (TCF) of -47.5 ppm/°C. The frequency drift is less than 1%.

Index Terms—AlGaIn/GaN HEMT, integrated high-temperature environmental sensors, integrated oscillator, lamb-wave.

I. INTRODUCTION

SMART sensors with integrated electronics that can operate at high ambient temperatures without external cooling can greatly benefit a variety of industrial applications, especially in automotive, aerospace and deep-well drilling [1]. For example, automobile engine and brake sensors are required to operate reliably at ambient temperatures above 150°C, telemetry during underground mining and oil drilling requires sensors and electronics to handle up to 225°C, and aircraft engine intelligent control and structural health monitoring systems with various sensors to function up to 500°C and higher [2], [3]. In such applications, monolithic integration of the sensor circuits with wireless transceivers would greatly reduce the system form factor, weight, and complexity. An essential component in these wireless sensor systems with high-temperature tolerance is a radio-frequency (RF) local oscillator possessing low-temperature dependence and coefficients. The RF carrier signal will be modulated by the sensor signal and transmitted to the cooler part of the system.

Comparing to their conventional counterparts such as silicon and GaAs technologies, circuits based on wide bandgap materials (GaN and SiC) offer superior performance under high-temperature environment. Recently, there have been several reported results of hybrid oscillators based on SiC operating at high temperatures ranging from 200°C to 475°C [4]–[6]. These oscillators used Cree’s SiC MESFETs mounted onto a substrate carrier. In addition, an NMOS SiC ring oscillator operating at

625 kHz under 300°C [7] and a 66 MHz, 375°C ring oscillator based on AlGaIn/GaN HEMTs on sapphire substrate [8] have also been demonstrated. However, these oscillators suffer from a relatively large temperature drift with large TCF on the order of 10^3 ppm/°C.

Crystalline III-nitride semiconductors offer many advantageous material properties, such as good piezoelectric property, high acoustic velocity, and inherent chemical inertness and thermal stability. Hence, it is suitable for fabricating surface acoustic wave (SAW) devices for harsh environmental sensing applications. High-sensitivity Lamb-wave sensors [9], [10] and a fully integrated SAW/HEMT oscillator [11] have recently been developed using GaN-on-Si structures.

In this letter, we demonstrate an on-chip GaN-based monolithic Lamb-wave oscillator on Si substrate for the first time. The 58 MHz oscillator operates at the lowest order anti-symmetric (A_0) mode. The high temperature characteristics of the A_0 wave were investigated in an open-loop delay line configuration, showing a superior temperature stability of the GaN-based Lamb-wave device (TCF of -62.6 ppm/°C). The integrated oscillator functions properly up to 250°C while maintaining a high output power of >11 dBm and a small TCF of -47.5 ppm/°C. Demonstration of this highly integrated device suggests the potential of monolithic GaN-based miniature sensor systems for high-temperature environments.

II. CIRCUIT DESIGN AND FABRICATION

A. Lamb-Wave Delay Line Oscillator Design

The Lamb-wave oscillator consists of an amplifier configured in a feedback loop with a Lamb-wave delay line. A five-stage HEMT amplifier was designed and each stage was an active-load common-source configuration, as illustrated in Fig. 1(a). Passive elements including metal-insulator-metal (MIM) capacitors and mesa resistors were fabricated on the same chip. On-chip bypass capacitors are also included for the gate (V_g) and drain (V_d) supplies, which are not shown in the schematic. The Lamb-wave delay line has a wavelength of $16 \mu\text{m}$, which determines the operation frequency of this oscillator. More details of the circuit design were given in [11].

B. Circuit Fabrication

The integrated oscillators along with individual device test structures were fabricated on an AlGaIn/GaN HEMT sample grown by metal-organic chemical vapor deposition (MOCVD) on a 2-inch (111) Si substrate. The structure consists of a thin AlN seed layer, a $1 \mu\text{m}$ GaN buffer layer with a thin interlayer in between, and an AlGaIn barrier layer. The fabrication process was modified from a conventional AlGaIn/GaN HEMT process flow. The electrode of the Lamb-wave device shared the same

Manuscript received February 24, 2013; accepted April 19, 2013. This work was supported by a grant (CA07/08.EG02) from the Research Grants Council.

The authors are with the Department of Electronic and Computer Engineering, The Hong Kong University of Science and Technology, Kowloon, Hong Kong (e-mail: eekmlau@ust.hk).

Color versions of one or more of the figures in this letter are available online at <http://ieeexplore.ieee.org>.

Digital Object Identifier 10.1109/LMWC.2013.2260734

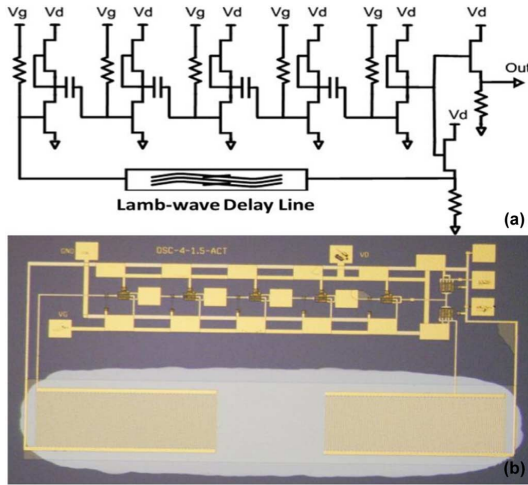


Fig. 1. (a) Circuit schematic and (b) micrograph of the integrated Lamb-wave oscillator.

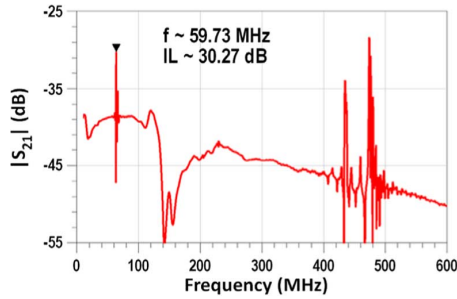


Fig. 2. Measured insertion loss ($|S_{21}|$) of the fabricated Lamb-wave delay line at RT.

metal layer with the HEMT gate electrode and the Si substrate was selectively removed from backside in the last step to release the Lamb-wave device membrane. Details of the layered structure and fabrication process have been reported in [10] and [11]. A micrograph of the fabricated circuit is shown in Fig. 1(b). The oscillator occupies an area of $2 \times 1.2 \text{ mm}^2$.

III. EXPERIMENTAL RESULTS

On-wafer high-temperature characterization of the devices and circuits was performed from RT to 250°C . A high-temperature probe station with a thermal controller to adjust and keep the temperature constant was used. The measurements were carried out in air ambient. Before each measurement, the temperature was held constant for 5 minutes to assure thermal equilibrium is reached.

A. Lamb-Wave Delay Line Characterization

The magnitude of S_{21} from 10 to 600 MHz of a Lamb-wave delay line in RT is plotted in Fig. 2. A sharp peak was clearly observed at 59.73 MHz with an insertion loss of 30.27 dB, which indicates the propagation of the A_0 mode wave. The corresponding phase velocity is $\sim 956 \text{ m/s}$ for the $16 \mu\text{m}$ wavelength and the $1 \mu\text{m}$ thick GaN-based membrane. This is in agreement with results using the numerical calculation suggested in [12]. The two other peaks at 435 and 474 MHz, are believed to be shear horizontal acoustic plate mode (SHAPM) and the lowest order symmetric mode (S_0) of acoustic waves, respectively. They are not included in this study.

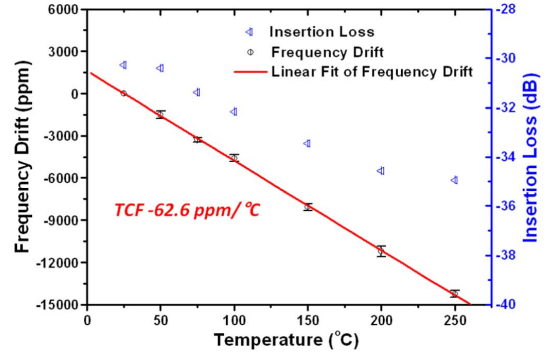


Fig. 3. Temperature dependence of the A_0 -wave peak frequency and insertion loss at the peak frequency.

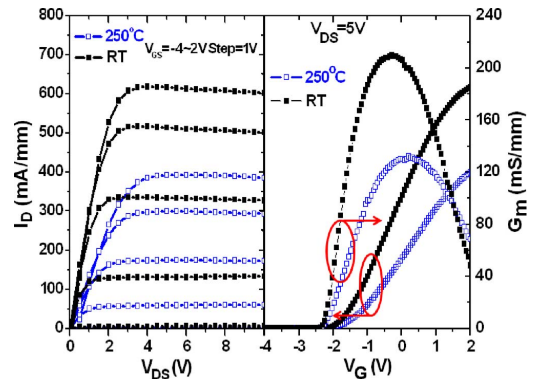


Fig. 4. DC characteristics of the AlGaIn/GaN HEMT at RT and 250°C .

The peak frequency drift and insertion loss of the A_0 wave are plotted as a function of temperature in Fig. 3. The peak frequency moves linearly with the temperature at a rate of $-62.6 \text{ ppm}/^\circ\text{C}$ and the insertion loss drops to -34.94 dB at 250°C . Three devices in the same wafer were measured and the fluctuations of the frequency drift were very small, within 380 ppm, as shown by the I-shaped error bars in Fig. 3. Given the different device configurations, the TCF of this GaN delay line device is somewhat larger than the reported value ($\sim -28 \text{ ppm}/^\circ\text{C}$) of the one-port AlN lamb-wave resonators [13], [14]. However, similar temperature-compensation technique, i.e., using SiO_2 , can be implemented in this GaN Lamb-wave device as well, to further improve the thermal stability. To our knowledge, this is the first reported high-temperature characterization for a GaN-based Lamb-wave device.

B. AlGaIn/GaN HEMT dc Performance

The measured typical dc characteristics of a D-mode HEMT are shown in Fig. 4. The device features a low dc output conductance and a peak transconductance (g_m) of 210 mS/mm with a threshold voltage of -2.1 V at RT. The devices in the amplifier path are sized to provide sufficient gain to satisfy the requirement for starting up the oscillation even at high temperature. At 250°C , the peak g_m decreased to 132 mS/mm , which sets the required device width to be $100 \mu\text{m}$.

C. Measured Oscillator Performance

The integrated oscillator oscillates at 58.58 MHz and produces an output power of 15.15 dBm at RT (Fig. 5), which matches well with the Lamb-wave delay line characteristics. As

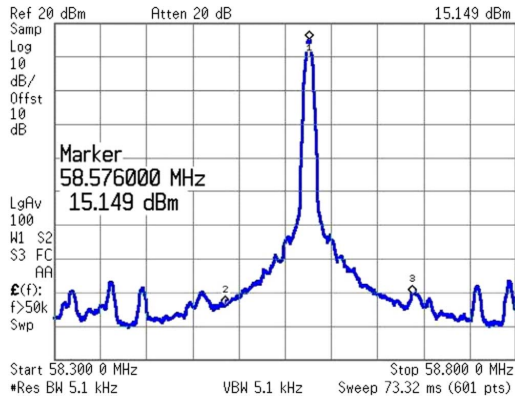


Fig. 5. Measured frequency spectrum of the integrated Lamb-wave oscillator operating at 58 MHz at RT.

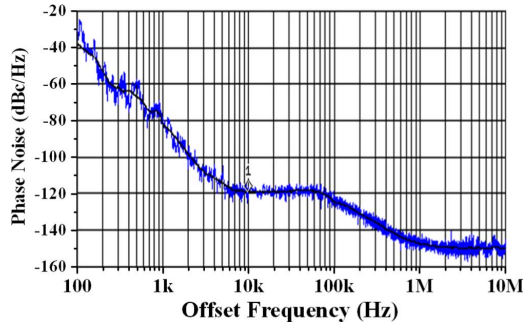


Fig. 6. Measured phase noise of the 58 MHz integrated Lamb-wave oscillator at RT.

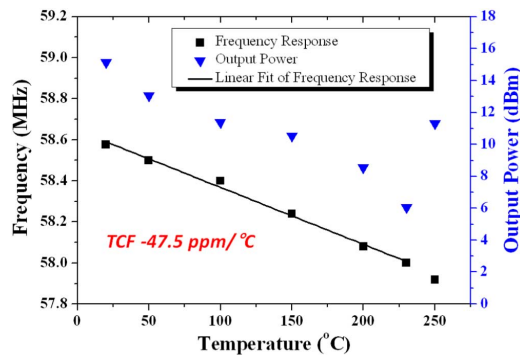


Fig. 7. Dependence of the oscillation frequency and the output power on temperature.

shown in Fig. 6, the measured phase noise of this 58 MHz oscillator at RT is -83 dBc/Hz at 1 kHz offset frequency and the phase noise floor is as low as -148 dBc/Hz. This oscillator design was chosen mainly for its simplicity to demonstrate the feasibility of monolithic integration and was not an optimized circuit for phase-noise performance. To further improve the phase noise, the amplifier configuration needs to be modified to a more complex topology.

Fig. 7 illustrates the dependence of the oscillation frequency and the output power on temperature. Over the temperature range from RT to 230°C and with a fixed bias condition, the oscillation frequency decreases linearly from 58.576 to 58.0 MHz, which is less than 1%. The TCF of the oscillator is -47.5 ppm/ $^\circ\text{C}$, which is lower than temperature dependence for the stand alone Lamb-wave delay line. This enhancement in TCF can be attributed to the feedback mechanism and the temperature dependence of the amplifier. By adjusting the gate

bias, oscillation up to 250°C (our measurement limit) was observable, with an output power of 11.3 dBm.

The performance of this oscillator is limited by both the increasing loss in the lamb-wave device and the decreasing gain in the HEMT amplifier at high temperatures. By optimizing the Lamb-wave device and designing a higher gain amplifier, or with better heat dissipation, the temperature performance could be further improved.

IV. CONCLUSION

For the first time, a monolithically integrated Lamb-wave oscillator operating up to 250°C has been developed using an AlGaIn/GaN-on-Si platform. The oscillation frequency exhibits a linear dependence on temperature with a small TCF of -47.5 ppm/ $^\circ\text{C}$. This work represents a major step toward the integration of GaN-based electronics with acoustic functions for high-temperature environmental sensing application.

ACKNOWLEDGMENT

The authors would like to thank A. Pan and Y. Chao for many helpful discussions and the staff of the Nanofabrication Facilities of HKUST for technical support.

REFERENCES

- [1] S. Lande and M. Research, "Supply and demand for high temperature electronics," in *Proc. 3rd Eur. Conf. High Temp. Electron. (HITEN 99)*, 1999, pp. 133–135.
- [2] R. W. Johnson, J. L. Evans, P. Jacobsen, J. R. Thompson, and M. Christopher, "The changing automotive environment: High temperature electronics," *IEEE Trans. Electron. Packag. Manufact.*, vol. 27, no. 3, pp. 164–176, Jul. 2004.
- [3] A. R. Behbahani, "Need for robust sensors for inherently fail-safe gas turbine engine controls, monitoring, and prognostics," in *Proc. 52nd Int. Instrum. Symp.*, Nov. 2006, [CD ROM].
- [4] G. E. Ponchak, M. C. Scardelletti, and J. L. Jordan, "30 and 90 MHz oscillators operating through 450 and 470 $^\circ\text{C}$ for high temperature wireless sensors," in *Proc. Asia-Pacific Microw. Conf. (APMC)*, 2010, pp. 1027–1030.
- [5] Z. D. Schwartz and G. E. Ponchak, "High temperature performance of a SiC MESFET based oscillator," in *IEEE MTT-S Int. Dig.*, Long Beach, CA, Jun. 12–17, 2005, pp. 1–4.
- [6] Z. D. Schwartz and G. E. Ponchak, "1-GHz, 200 $^\circ\text{C}$, SiC MESFET Clapp oscillator," *IEEE Microw. Wireless Compon. Lett.*, vol. 15, pp. 730–732, 2005.
- [7] U. Schmid, S. T. Sheppard, and W. Wondrak, "High temperature performance of NMOS integrated inverters and ring oscillators in 6H-SiC," *IEEE Trans. Electron Devices*, vol. 47, pp. 687–691, 2000.
- [8] Y. Cai, Z. Cheng, Z. Yang, C. W. Tang, K. M. Lau, and K. J. Chen, "High-temperature operation of AlGaIn/GaN HEMTs Direct-Coupled FET Logic (DCFL) integrated circuits," *IEEE Electron Device Lett.*, vol. 28, pp. 328–331, 2007.
- [9] A. K. Pantazis, E. Gizeli, and G. Konstantinidis, "A high frequency GaN lamb-wave sensor device," *Appl. Phys. Lett.*, vol. 96, p. 194103-3, 2010.
- [10] X. Lu, C. M. Lee, S. Y. Wu, H. P. Ho, and K. M. Lau, "GaN-based S_0 -wave sensors on silicon for chemical and biological sensing in liquid environments," *IEEE Sensors J.*, vol. 13, no. 4, pp. 1245–1251, Apr. 2013.
- [11] X. Lu, J. Ma, X. Zhu, C. M. Lee, C. P. Yue, and K. M. Lau, "A novel GaN-based monolithic SAW/HEMT oscillator on silicon," in *Proc. IEEE Int. Ultrason. Symp.*, Oct. 2012, [CD ROM].
- [12] M. J. Vellekoop, *A Smart Lamb-Wave Sensor System for the Determination of Fluid Properties*. Delft, The Netherlands: Delft Univ. Press-III, 1994, p. 31.
- [13] C.-M. Lin, T.-T. Yen, Y.-J. Lai, V. V. Felmetzger, M. A. Hopcroft, J. H. Kuypers, and A. P. Pisano, "Temperature-compensated aluminum nitride lamb wave resonators," *IEEE Trans. Ultrason., Ferroelectr. Freq. Control*, vol. 57, pp. 524–532, 2010.
- [14] M. Rinaldi, A. Tazzoli, J. Segovia-Fernandez, V. Felmetzger, and G. Piazza, "High power and low temperature coefficient of frequency oscillator based on a fully anchored and oxide compensated AlN contour-mode MEMS resonator," in *Proc. 25th IEEE Int. Conf. Micro Electro Mech. Syst. (MEMS'12)*, 2012, pp. 696–699.